X-ray absorption near-edge structure calculations beyond the muffin-tin approximation

Y. Joly
Laboratoire de Cristallographie, Centre National de la Recherche Scientifique, Associé à l'Université Joseph Fourier, Boîte Postale 166, F-38042 Grenoble Cedex 9, France

(Received 3 August 2000; revised manuscript received 21 November 2000; published 13 March 2001)

A new scheme for calculating the x-ray absorption near edge structure (XANES) based on the finite-difference method is proposed. It allows completely free potential shape and, in particular, is not constrained to the muffin-tin approximation. In our approach, the calculation of the final states is performed in real space. The Schrödinger equation is solved in a discrete form on the node points of a three-dimensional grid. The unknowns are the values of the wave functions at the grid points. The validity of the method is shown on two different systems the metallic copper and the carbon monoxide molecule; then, the differences resulting from muffin-tin and non-muffin-tin calculations are shown on different typical molecules.

DOI: 10.1103/PhysRevB.63.125120 PACS number(s): 78.70.Dm, 71.20.Ps

I. INTRODUCTION

A number of spectroscopies are related to the transition process of a core electron to some upper empty level. The success of such spectroscopies is due to the fact that the photoelectron is an efficient localized probe around a specific atom. Due to the final state selection rules, these spectroscopies selectively probe the empty valence states allowing analysis of electronic as well as crystallographic structure. When calculating these spectra, the main difficulty is the evaluation of the final state. The initial state is a core state and so is easy to calculate. The transition operator connecting the initial and final states can also be well approximated.

Among, these techniques, the most used is extended x-ray absorption spectroscopy (EXAFS). Over 50 eV above the rising edge an important approximation can be made. The region around the excited atom is spherically averaged so the photoelectron wave function can be constructed as a simple superposition between an outgoing spherical wave and a wave backscattered by the neighboring shells of atoms. Unfortunately at lower energy, this single scattering approximation is not valid and many processes contribute in a non-negligible way: many body effect, multiple scattering (MS) effect, polarization effect, and so on. These calculations are then a formidable task, nevertheless they are important because it is at these energies that the signal is very sensitive to the three-dimensional (3D) crystallographic, electronic and magnetic structures.

The x-ray absorption near edge structures (XANES), is the domain of XAS extending up to around 50 eV above the threshold. Different approaches are used to calculate these final states. A first group of them turns around the work of De Groot[1] using the framework of atomic multiplets for the absorbing atom in crystal field. The second approach uses the local density approximation to calculate the final states. This is done considering infinite crystals[2] (a band structure approach) or clusters using the multiple scattering theory.[3,4] Typically, MS theories employ an important approximation: the muffin-tin averaging of the potential needed for the expansion of the wave functions. In this latter approximation, the potential is spherically averaged in the atomic and outer-sphere regions and volume averaged in the interatomic region. The use of a constant interstitial potential is certainly a serious approximation, specially when the photoelectron kinetic energy is close to the value of the approximation done on the potential. Moreover, it makes the results depend on the size of the interstitial region itself. As shown in Ref. 5, the restrictions imposed by the muffin-tin approximation can be lifted through a generalization of the multiple-scattering theory. Some works, which can be applied to XANES, have already tried to go beyond the muffin-tin approximation for energy band problems. In particular, the discrete variational method[6] uses a discretization of the potential to calculate matrix elements but keeps the usual expansion in plane waves in its Koringa-Kohn-Rostoker version. Ebert and co-workers[7] using also the Koringa–Kohn–Rostoker formalism in a full potential approach have successfully applied the formalism to XANES.[8–10] The full linear augmented plane wave (FLAPW) approach[11] is also extensively used to calculate band structure without the muffin-tin approximation, but all of these methods are restricted to periodic potential.

The finite-difference method (FDM) is another way to solve the Schrödinger equation using the local density approximation which avoids the muffin-tin approximation. The first formulation of FDM to solve the Schrödinger equation was given in the 1930s.[12] The FDM requires significant computing power and its progress has followed the improvements of computer-capabilities. One of its first satisfactory application in the field of solid state physics concerns the binding energy states by Puska and Nieminen in 1983.[13] Very recently the first FDM band structure calculation was reported.[14] In two letters, the technique was extended to low-energy electron diffraction[15] and low-energy positron diffraction.[16] The sensitivity of low energy particles on electronic parameters and consequently on the muffin-tin approximation was illustrated in Ref. 17. The purpose of the present article is first to describe the extension of this computing technique to XANES and related spectroscopies and to show in typical examples the potentiality of the method and second to analyze the improvements to XANES calculations due to the better description of the potential.

II. XANES AND RELATED SPECTROSCOPIES

In the one-electron quadrupolar approximation, and neglecting spin for simplicity, the transition amplitudes be-

tween an initial core state ψ_g and a final state ψ_f are given by

$$M_{gf}=\left\langle \psi_f \left| \boldsymbol{\varepsilon}\cdot\mathbf{r}\left(1+\frac{i}{2}\mathbf{k}\cdot\mathbf{r}\right)\psi_g \right\rangle,$$

for photons with wave vector $\mathbf{k}$ polarized in the $\boldsymbol{\epsilon}$ direction. For XANES, the photoabsorption cross section is then given by

$$\sigma=4\pi^2\alpha\hbar\omega\sum_{f,g}|M_{gf}|^2\delta(\hbar\omega-E_f+E_g),$$

where α is the fine structure constant, $\hbar\omega$ the photon energy, and E_f and E_g the final and initial state energies, respectively. For circularly polarized photons, the expression remains the same, but the polarization is complex. For diffraction anomalous fine structure (DAFS), the transition is virtual and one has to make the distinction between the incident and scattered polarization and wave vector and corresponding transition amplitudes M^i_{fg} and M^s_{fg}. The amplitude emitted by one atom is then

$$A=(\hbar\omega)^2\sum_{f,g}\frac{M^{i*}_{gf}M^s_{gf}}{E_f-E_g-\hbar\omega+i(\Gamma/2)}.$$

The total amplitude is obtained through the summation over the atoms at position $\mathbf{R}_a$, as in XANES, but weighted by the phase factor $e^{i(\mathbf{k}_i-\mathbf{k}_s)\mathbf{R}_a}$.

In the *ab initio* calculation the difficulty resides in the evaluation of the final states. The initial state can be represented by an atomic core orbital which is easy to calculate and the evaluation of the matrices M_{gf} followed by the summation over the final states to get absorption cross section or diffracted intensities is straightforward. It is the evaluation of these final states which is performed through the finite difference method.

III. THE FINITE DIFFERENCE METHOD

The FDM is a general way to solve differential equations by discretizing them over a grid of points in the whole volume where the calculation is made. In XANES, we are interested in the Schrödinger equation in a spherical volume centered on the absorbing atom and extending over a sufficiently large cluster.

In the ''discretized'' version of the equation, the unknowns become the values of the wave function on each grid point ''*i*'': $\psi_i=\psi(\mathbf{r}_i)$. The way to calculate the potential on the node points $V_i=V(\mathbf{r}_i)$ will be seen further on. The Laplacian is obtained by approximating the wave function around the point *i* by a polynomial of fourth order. The fourth order calculation is more economical than the second order one. Then the Laplacian is given by

$$\Delta\psi_i=\frac{1}{h^2}\left(\frac{4}{3}\sum_{j,\varepsilon}\psi^{\varepsilon}_j-\frac{1}{12}\sum_{j,\varepsilon}\psi^{\varepsilon\varepsilon}_j-\frac{15}{2}\psi_i\right),$$

where ψ^{ε}_j and $\psi^{\varepsilon\varepsilon}_j$ with $\varepsilon=-$ or $+$, are the values of the wave function on the first and second neighboring points on the grid in the directions εj. h is the distance between the points.

At the end, denoting l_{ij} the Laplacian operator, one gets for the Schrödinger equation on point ''*i*:''

$$(-l_{ii}+V_i-E)\psi_i+\sum_{j}^{\text{neighbors}}-l_{ij}\psi_j=0 \qquad (1)$$

expressed in Rydbergs and atomic units. Finally, a large system of linear equations connects the values of the wave function on all points ''*i*.'' With a smaller interpoint distance, the computation is more accurate.

IV. APPLICATION TO XANES CALCULATION

A. The areas of calculations

The wave function must be calculated in all the area centered around the absorbing atom extending sufficiently far from it where the backscattered wave function do not give more contribution to the scattered wave field on the absorbing atom. Thus the area of calculation is limited by an outer sphere where the potential is assumed constant or at least with a spherical symmetry. There, an expansion in spherical waves is performed.

Inside this sphere the classical FDM equation is used. Nevertheless, close to the ion core, the kinetic energy of the electron is very high, whereas in the region between two ion cores, it is much lower. Consequently, it can appear as necessary to use a non uniform grid points to solve the Schrödinger equation as was proposed in an other paper.[15] A less CPU consuming solution is now preferred. It consists in performing an expansion in spherical waves in very little sphere around the atomic cores, providing the fact that the potential is quite spherically symmetric in these areas. Note that these spheres are much smaller spheres (up to 0.5–0.7 Å, depending of the atoms) than the spheres in a muffin-tin formulation. A second advantage of this framework is that the expansion in spherical harmonics, particularly in the excited atom, is specially convenient for calculating the matrix transition amplitudes. These areas, as the outer sphere, are coupled to the interatomic FDM grid through equations given further on.

B. The atomic core

In the atomic core, the potential can be represented as a multipole expansion around the center:

$$V(\mathbf{r})=\sum_{L}V_L(r)Y_L(\Omega), \qquad (2)$$

r being the radial distance to the center of the atom and Ω the angular position. L stands for (l,m). The real spherical harmonics $Y_L(\Omega)$ are defined following Condon and Shortley.[18]

The general solution $\psi(\mathbf{r})$ in the atomic sphere can be expressed as a linear combination of independent solutions of the Schrödinger equation:

$$\psi(\mathbf{r}) = \sum_L a_L \phi_L(\mathbf{r}). \tag{3}$$

Each of these independent solutions is expanded in the same way as the potential:

$$\phi_L(\mathbf{r}) = \sum_{L'} \varphi_{L'L}(r) Y_{L'}(\Omega).$$

They are defined by their regular component near the origin:

$$\varphi_{LL'}(r) \cong r^l \delta_{LL'}.$$

Inserting these expansions into the Schrödinger equation and using the orthogonality of the spherical harmonics, we find that the functions $\varphi_{L'L}(r)$ satisfy the following set of coupled differential equations:

$$\left[\frac{1}{r^2}\frac{d}{dr}\left(r^2\frac{d}{dr}\right) + E - \frac{l'(l'+1)}{r^2}\right]\varphi_{L'L}(r) = \sum_{L''L'''} C^{L'}_{L''L'''} V_{L''L'}(r)\varphi_{L''}(r). \tag{4}$$

The $C^{L'}_{L''L'''}$ are the real Gaunt coefficient:

$$C^{L'}_{L''L'''} = \int Y_{L''}(\Omega) Y_{L'}(\Omega) Y_{L'''}(\Omega) d\Omega.$$

Now, as stated above, the atomic spheres are not the usual muffin-tin sphere, but smaller sphere. Most often, as is demonstrated further in the paper, the potential can there be taken as completely spherical and the multipolar expansion of the potential (2) is reduced to the first term. In such cases, the nonzero $\varphi_{LL'}$ are the diagonal components ($L = L'$).

The unknowns are the amplitudes a^f_L of these harmonics. They are evaluated together with the value of the wave function on all the node points of the FDM grid using the continuity of the wave function between the different zones and an ''approached'' Fourier transform. The continuity is used in Eq. (1) for the points at the boundary of the atomic spheres. For these points, one or several neighboring points are entirely within the inner sphere (Fig. 1). Thus one replaces the unknown ψ_j by the expansion (3) with its new unknowns a^f_L. Of course one needs new equations to find these new unknowns. To this end, we use again Eq. (3) applied over the points at the sphere boundary (white in Fig. 1). Having the continuity in two crowns of points inside and just outside the sphere one gets the continuity of the derivative. In order to get the same number of equations as unknowns, one proceeds in the same way as for a Fourier transform. That is, for each spherical harmonic, one integrates Eq. (3) after multiplication by the Y_L, over the sphere:

$$\sum_i^{\text{white.pt}} Y_{L,i}\psi_i d\Omega_i = \sum_{L'} a^f_{L'}\left(\sum_i^{\text{white.pt.}} Y_{L,i}\phi_{L',i} d\Omega_i\right). \tag{5}$$

The $d\Omega_i$ are weights related to the solid angles occupied by the points. In practice one chooses

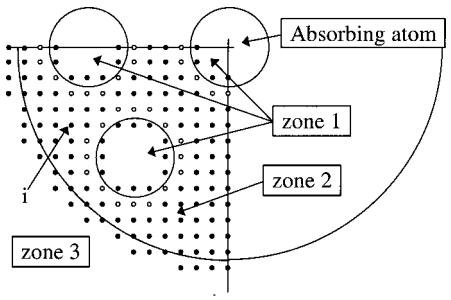

FIG. 1. General view of the meshing in the whole region of calculation around the absorbing atom. Symmetry planes are used to reduce the area of calculation. This one is divided in three zones: (1) around the atomic cores, (2) between the atoms where the standard FDM calculation is used, (3) the outer sphere region. ''*i*'' is the index of a point where formula (1) matching this point to its neighbors can be directly applied. White points are at the boundary of the ion core. It is on these points that is used the formula (5) to embed the atom in the FDM grid. Gray points are at the boundary of the outer sphere. Formula (7) is applied on these points to match the FDM grid to the continuum.

$$d\Omega_i = 4\pi \frac{dv_i}{\Sigma_i dv_i},$$

where dv_i is the volume occupied by the point *i*. For a point in a general position this volume is h^3, h being the interpoint distance. When a symmetry plane crosses this point, its volume is divided by 2. This would be a Fourier transform if the interpoint distance was infinitely small. This kind of embedding is close to the one proposed by Thijssen and Inglesfield.[14]

C. Connection with the continuum

In the outer sphere, the potential is constant and the solutions are the Neumann and Bessel (or Hankel) functions (note that one could use in this area the functions resulting from Coulomb potential). So the general solution in this region is given by

$$\psi^f(\mathbf{r}) = J_{L_f}(\mathbf{r}) + i\sum_L \tau^f_L H^{(1)}_L(\mathbf{r}), \tag{6}$$

where J_L and $H^{(1)}_L$ are the generalized Bessel and Hankel functions. These functions are related to the classical Hankel, $h^{(1)}_l$, and Bessel functions through, for instance, for the Hankel one:

$$H^{(1)}_L(\mathbf{r}) = \sqrt{\frac{\sqrt{E - V_m}}{\pi}} h^{(1)}_l(r) Y_L(\Omega),$$

V_m is the averaged potential in the outer sphere. r and Ω are the radial and angular positions, the origin being placed at the center of the sphere defining the area of calculation. Note that this center is not necessarily the center of the absorbing atom. The unknowns are the amplitudes τ^f_L. It is important to note the normalization of the Hankel functions which comes from the density of state in the vacuum. This normal-

ization implies by continuity, all the normalization in the different regions of calculation. In practice, if there is no damping, that is when the self-energy is real, it is less CPU and memory consuming to work with a real base, that is using the Bessel–Neuman normalization instead of the Bessel–Hankel one:[19]

$$\psi^f_{\text{bessel-neuman}}(\mathbf{r}) = J_{L_f}(\mathbf{r}) + \sum_L \eta^f_L N_L(\mathbf{r})$$

N_L, being the generalized Neuman function. Then the renormalization is given by

$$\psi_{\text{bessel-hankel}} = \frac{1}{1+i\eta}\psi_{\text{bessel-neuman}}.$$

The matching between the interatomic area and the outer sphere is performed exactly in the same way as between the inter-atomic area and the atomic core spheres. From this, we can derive

$$\sum_i^{\text{gray.pt}} Y_{L,i}\psi_i d\Omega_i = i\sum_{L'} \tau^{L_f}_{L'}\left(\sum_i^{\text{gray.pt.}} Y_{L,i}H^{(1)}_{L',i}d\Omega_i\right) + \sum_i^{\text{gray.pt}} Y_{L,i}J_{L_f,i}d\Omega_i. \quad (7)$$

The summation is over the gray points (see Fig. 1) that are at the boundary of the outer sphere. It must be noticed that because the radius of this sphere is larger than the atomic core ones, we need here far more spherical harmonics. For typical calculation (up to 6, 7, or 8 Å) we need a maximum second quantum number value, $l_{\max}$ of at least 20 or 30.

D. Potential

Having written the Schrödinger equation on all points of the grid, the potential must be introduced in the general matrix. As usual in standard XANES calculations, the local density approximation is used to calculate the potential. When neglecting the core hole effect, the electronic density can be calculated in a self consistent way in a periodical system using a band structure program, as the LAPW method.[11] When structures are too complicated to be confidently calculated self-consistently, or when we are interested in the investigation of specific phenomena as orbital ordering, charge ordering, core hole screening, etc. ..., an independent way of constructing the electronic density is more useful. In that way, the first step is making a simple superposition of atomic densities with a controlled occupancy of each orbital of each atom.[20,21] It is then possible to improve further the calculation by considering bonds or any kind of electronic rearrangement.[17] This has already be done in our formalism to study orbital ordering in manganites[22] and in V_2O_3.[23] Nevertheless, it can be already noted that the electronic density depends on the choice of the occupied atomic orbitals. Several choice are offered as the use of the Clementi and Roetti bases.[24] Note that in most XANES calculations, the atoms are taken as neutral with orbital bases corresponding to neutral atoms. The Coulomb potential is then calculated solving the Poisson equation and the energy dependant exchange-correlation potential is obtain following the Hedin and Lundqvist[25] approach.

The FDM formulation allows no approximation of the shape of the potential, thus avoiding the problem related to the classical muffin-tin approximation. So starting from the potential calculated as described above and as in other programs, no other approximation, contrary to most of the other formalisms, is superimposed. The object of the present study, apart of describing the formalism and proving its validity, is to make comparisons of calculations with and without the muffin-tin approximation. So in that work, the simple superposition scheme of atomic densities is kept and special attention is given on the effect of the muffin-tinisation of the resulting potential.

At this stage, one can immediately remark than a lot of studies already done on the choice of the exchange correlation potential would have to be done again without the muffin-tin approximation because this approximation could artificially improve one model over the others. That point is nevertheless beyond the scope of this paper.

E. General matrix

From the preceding steps, one gets the general matrix, which includes the n_p Schrödinger equations (1) on the n_p points of the FDM grid and the ''approached'' Fourier transform around the ion cores [formulas (5)] and the outer sphere [formula (7)]:

$$\begin{bmatrix} A_1 & B_1 & & & & & & & & \\ C_1 & H & N & & & & & 0 & & \\ & N & H & N & & & & & & \\ & & N & H & C_2 & & & & & \\ & & & B_2 & A_2 & B_2 & & & & \\ & & & & C_2 & H & N & & & \\ & & & & & & \cdot & & & \\ & & & & & & & \cdot & & \\ & & & & & & & \cdot & & \\ & 0 & & & & & & N & H & C_0 \\ & & & & & & & & B_0 & A_0 \end{bmatrix} \times \begin{bmatrix} a^f_{L1} \\ \psi^f \\ \cdot \\ \cdot \\ a^f_{L2} \\ \psi^f \\ \cdot \\ \cdot \\ \cdot \\ \cdot \\ \tau^f_L \end{bmatrix} = \begin{bmatrix} 0 \\ 0 \\ \cdot \\ \cdot \\ 0 \\ 0 \\ \cdot \\ \cdot \\ \cdot \\ MJ^f \\ GJ^f \end{bmatrix}.$$

The (N, H, N) submatrices contain the coefficients of FDM equation (1). The N submatrix is substituted by the C submatrix when a missing neighbor is encountered using in that case formulas (4) or (6). The ''approached'' Fourier transforms correspond to the submatrices A_a and B_a, a being the

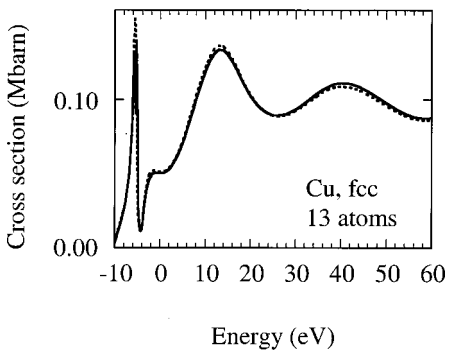

FIG. 2. *K* edge XANES spectra of copper for a 13 atoms cluster. MS (dotted line) and FDM (full line) calculation gives quite similar results.

index of the atom, *o* standing for the outer sphere. They are implemented in order to get a matrix band width as small as possible. The second member of the linear system of equations is given by the connection to the outer sphere through the formulas (6) and (7) giving MJ^f and GJ^f. The system can then be solved and the amplitudes of the final states extracted to calculate the photoabsorption cross section. Note that this is a non hermitian band matrix and that only the second member depends on the final state.

V. TESTING THE METHOD

Having given the general framework, one has to prove its practical use in some typical examples. For this purpose, the method was applied to three very different classes of material: dense metals, molecules and oxides. Works on oxides being already published,[20,21,26] we refer to these papers to check the quality of the experimental-theory agreement which can be reached in this class of compound. Results will be given in the next section on the *K* edges of copper in its fcc pure structure and carbon in the CO molecule. Calculations on copper are also used to check the different technical parameters necessary in the FDM formalism.

A. Validity of the method

To prove that the FDM approach is able to calculate XANES, one may compare with the multiple scattering approach in a situation where the muffin-tin approximation is presumably valid. The building of the potential can be slightly different between the different XANES programs already available. So, to get confident comparison between MS and FDM calculations, both approaches are included in the same code, the only difference in the potential being its ''muffin-tinisation.''

As a test case, a cluster of 13 copper atoms is chosen, that is the central absorbing atom plus its first surrounding shell embedded in the fcc crystal. Figure 2 shows the comparison of the FDM and MS calculations. The curves are quite similar. The equivalence of the results shows together with the validity of the FDM method that non-muffin-tin calculations are really not necessary in highly symmetrical dense metal! The maybe surprising element is that an interpoint distance *h* of 0.25 Å is sufficient to reach such agreement. Few minutes on a PC are sufficient in this highly symmetrical case to calculate the spectra.

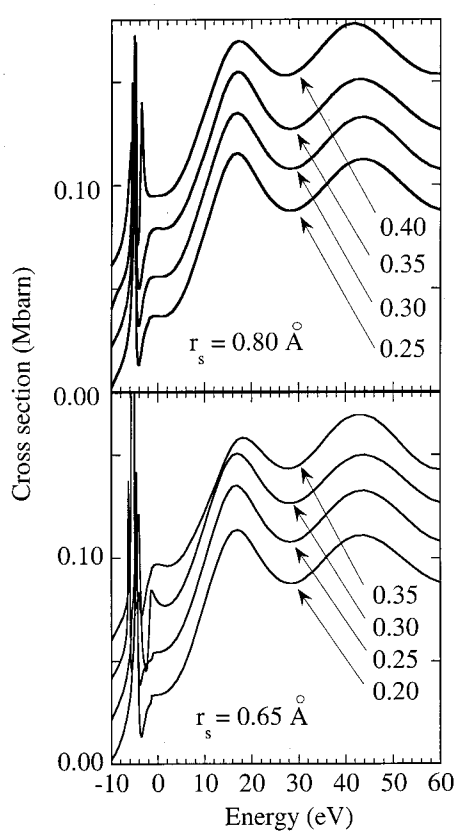

FIG. 3. Study of the convergence of the calculation versus the inter-point distance. Top, the ion core sphere radius r_s is 0.80 Å and convergence is reached at $h=0.30$ Å. Bottom, $r_s=0.65$ Å and convergence is reached at $h=0.25$ Å. $l_{\max}$ is limited to 5. The occupied states are not subtracted.

B. Convergence

Now to check convergence, different calculations for *h* going from 0.20 to 0.40 Å were performed both in second- and fourth-order approximations. These calculations are also performed at different values of the ion core sphere radius r_s, where the expansion in spherical wave is done. The spectra are shown in Fig. 3. The occupied states are not subtracted. It can be checked that for $r_s=0.80$ Å and at fourth order, residual differences are very small with $h=0.35$ Å. Convergence is completely reached at 0.30 Å in all the energy range up to 60 eV. With $r_s=0.65$ Å, a 0.25 Å interpoint distance is needed. This is due to the fact that the potential at this distance from the center of the atomic core is greater. Note that at high value of the interpoint distance, the number of points around the atom necessary for the connection to the expansion in spherical waves in the atoms must remain substantially greater than the number of spherical harmonics otherwise numerical instabilities can appear. For this reason, $l_{\max}$ in this calculation is limited to 5.

Thus we assess that convergence in the typical XANES energy range is reached with interpoint distance values close

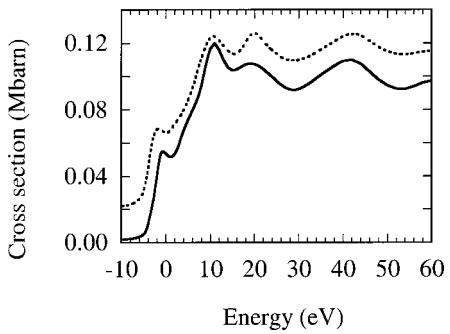

FIG. 4. *K* edge XANES spectra of copper for a 141 atoms cluster. Experiment (dotted line) and FDM calculation (full line).

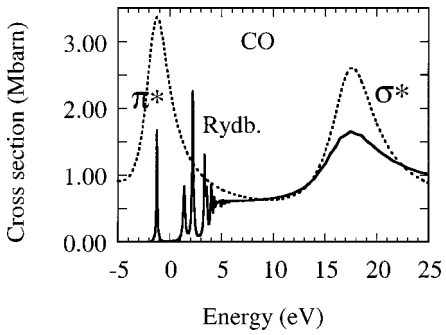

FIG. 5. *K* edge XANES spectra of carbon in CO FDM calculation: full line, MS calculation: dotted line. Bounded π^* and not bounded states σ^* are reproduced. Rydberg series are also present in the FDM calculation.

to 0.25 Å at order four. That gives around 16 000 points for a 3.9 Å radius cluster, and 32 000 points for a 4.9 Å radius cluster. Using symmetries to reduce the area of calculation, these numbers are divided by 2, 4, 8, or 16. Such symmetrical calculations which needs typically 250 Mo of memory space can be done in some hours on conventional PC and this up to the conventional useful cluster radius in XANES that is 8 Å. In more general situation when few symmetries are present the needed space memory grows up to several gigaoctet. In these situations calculations are tractable on vectorial computers.

Convergence versus the number of shells where checked in both approaches, muffin-tin MS and non-muffin-tin FDM. With a 8.3 Å radius cluster and 141 atoms, convergence becomes satisfying. It can be seen in Fig. 4 that both approaches gives again very close results.

C. Testing the multipolar expansion in the ion core sphere

Calculations using different radii for the ion core sphere were performed using multipolar or monopolar expansions of the potential in the spheres. At the end, all of these calculations give very similar results. This is not surprising for copper where the validity of the muffin-tin approximation is well established and verified just above. That means that a monopolar expansion is sufficient up to the muffin-tin radius, that is 1.28 Å (without overlaping). A monopolar expansion is obligatory sufficient for our low r_s value.

The CO case is more interesting because, due to his lower symmetry, an $l=1$ term in the multipolar expansion is already nonzero (for copper, after the spherical component, the first non zero term is for $l=4$). In that case multipolar and monopolar calculations were performed with $r_s=0.5$ Å (to compare with the inter atomic distance 1.13 Å). Again, results are very similar.

So, we prove that in both classes of material, the monopolar potential component is sufficient to describe the scattering by the ion core sphere providing its radius remains notably smaller than the half-interatomic distance. The only cases where this conclusion would have to be verified concern heavy, low symmetrical atoms.

D. Checking bonding states and Rydberg series

A very simple molecule is chosen to check the validity of the FDM mode of calculation in an another class of compound, that is a little organic molecule exhibiting molecular localized antibonding orbitals, Rydberg series, and orbitals in the continuum (Fig. 5).

Calculations were done, as above, with electronic density resulting from the simple superposition of atomic orbitals but with the atomic charges provided by a Mulliken analysis in the Gaussian package[27] (+ and −0.29 on the carbon and oxygen). At this stage, the increase of population between the atoms due to the covalence was not taken into account but this can be done as it was shown using the same frame.[16]

Multiple scattering and finite-difference method calculations are shown in the figure. The antibonding π^* and σ^* are present at the good energies. To get the cross section to fall to zero between them, the radius of the outer sphere must be sufficient (3 Å). The addition of an outer sphere with a $1/r$ potential is necessary to get the Rydberg series. The MS calculation could be improved to also get the Rydberg series. With this result, we prove that the FDM is able to calculate in a same run XANES spectra in molecules presenting unoccupied bounded states together with the continuum states.

VI. STUDY OF THE VALIDITY OF THE MUFFIN-TIN APPROXIMATION

A. About the muffin-tin calculations

The muffin-tin approximation corresponds to a monopolar representation of the potential. The potential in the interstitial region is constant. Very often, overlapping muffin-tin spheres are used to take into account a part of the scattering power of the interstitial area. The use of overlapping spheres is mathematically wrong but up to reasonable values of the overlap that is 10% or 15%, the benefit remains greater than the error. It must be noticed that relatively good artificial agreement can even be reached in some cases playing with the interstitial potential and the muffin-tin radius. These false improvements can hide structural or electronic informations.

As seen before, in a highly symmetrical system, the first nonzero term in the multipolar expansion of the potential (a part the spherical one) corresponds to the azimuthal quantum number $l=4$ (as in the copper fcc structure). This fact also concerns the interstitial area in case of overlap. The number of spherical harmonics necessary to describe the wave scattering by an atom of radius R is given by the maximum value of l: $l_{\max}=kR$, typically 3–6. The spherical expansion of the

Schrödinger equation (4) shows that the coupling terms between the different harmonics are related to the multipolar expansion of the potential. With few multipolar terms in the l range of the wave expansion, it is not surprising that the muffin-tin approximation be very good. The monopolar expansion of the potential is sufficient even in the overlapping part of the muffin-tin spheres and so the interstitial region is rather well described. Naturally, this is specially true when the system is dense, because the interstitial region is there anyway sufficiently small to be described by a constant potential.

To have the best possible MS muffin-tin calculation, a specific attention is given on the choice of the muffin-tin radius and on the value of the interstitial potential. Over the conventional assessment where it is stated that this last is the average of the potential in the interstitial region, this interstitial region is not easy to define in the case of nonperiodic material. For the muffin-tin radius, very often the Norman procedure is chosen. The radius is then related to the expansion of the atomic electronic density.[28] A better choice is to work directly on the potential. The best radius is the one which minimizes the potential jump between the sphere and the interstitial area. It is what we choose here. The second point is around the muffin-tin overlap. A quite standard procedure is to work with a 10% to 15% overlap, because it has empirically been observed that it is with such overlap that the agreement with experiment is often the best. For the following we verified that the 10% overlap best agrees (or is the less different) with the non-muffin-tin calculations. So the MS calculations presented in the next sections use this overlap. The comparisons are there between FDM and MS calculations. Thus they show the difference between non-muffin-tin (or full) potential and an improved (because overlapping) muffin-tin potential.

B. Decreasing the symmetry

From the considerations above, it can be suspected that decreasing the symmetry, non muffin-tin effect must increasingly influence the signal. To check this assumption, numerical tests on small artificial iron–oxide molecules are realized. No special attention is given to the atomic charges or interatomic distances because the purpose is not to compare to an experiment but only to evaluate the difference between muffin-tin and non muffin-tin calculations.

FeO_6 *octahedra*

Calculations on ordered and distorted FeO_6 octahedra are performed. In Fig. 6, the calculations for the perfect octahedron are shown. The Fe–O distance is 2 Å and the O–Fe–O angles are 90°. The symmetry is cubic and the agreement between MS and FDM is very good.

Then the octahedron is contracted along the z axis by 10%. There is a loss of 2 fourfold axes, the iron remains a center of symmetry. Figure 7 shows the linear dichroism between the polarization parallel and perpendicular to the contraction. The difference between MS and FDM is noticeable in the 0–50 eV range. Comparing with the nondistorted octahedron spectra in Fig. 6, it can be checked that MS underestimates the effect of this contraction and thus a fit on this parameter would give an error of around 20%.

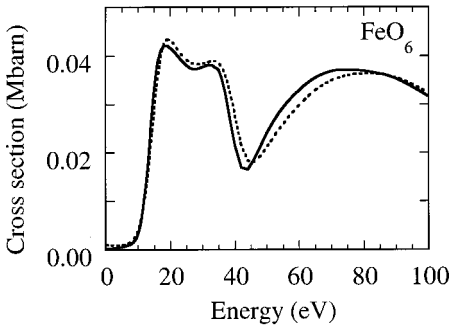

FIG. 6. Fe K edge in the perfect FeO_6 octahedron. Interatomic distance is 2 Å. Full line: FDM dotted line: MS.

The loss of center of symmetry is very important for many physical phenomena. The use of XANES to analyze it can be fruitful if its calculation is sufficiently precise. So calculations are now performed for a FeO_6 molecule, keeping the perfect oxygen octahedron, but the iron being displaced by 0.1 Å toward the apical (along Oz) oxygen. The linear dichroism is stronger (Fig. 8). The large first peak for polarization along z, due to this loss of symmetry, is present in both MS and FDM calculations. The differences are more located in the edge region. When the polarization is perpendicular to the iron displacement, the FDM calculation gives a sensitivity to this displacement. On the contrary, the MS calculation is quite similar with the displaced or not displaced iron (Fig. 6).

Asymmetrical oxides

More asymmetrical situations occurs when the first atomic shell is not complete around the absorbing atom. For instance at a surface, the atoms of the first atomic plane have no neighbor in the vacuum direction. It is what we roughly illustrate with calculations on a FeO_5 molecule, where from

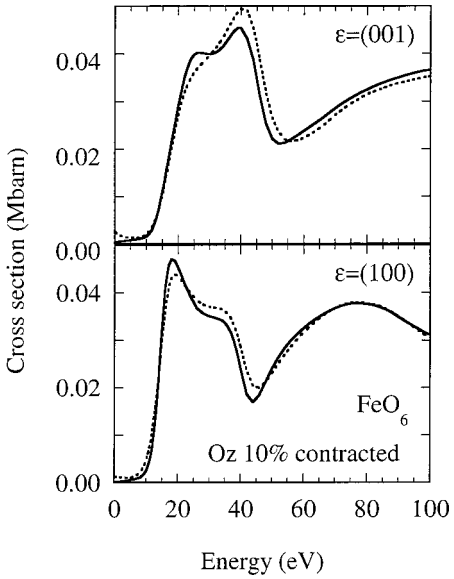

FIG. 7. Fe K edge in the contracted FeO_6 octahedron. The contraction is 10% along Oz. Full line: FDM, dotted line: MS.

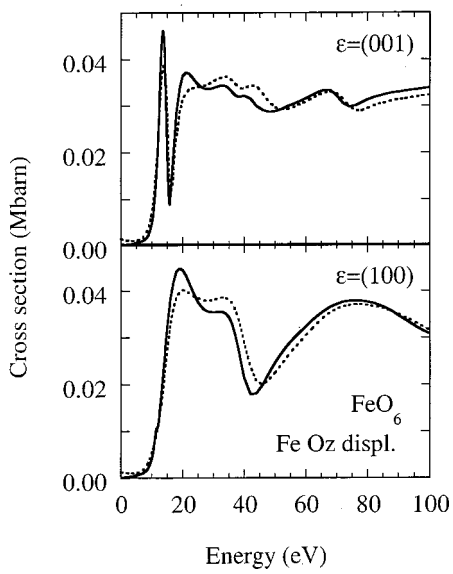

FIG. 8. Fe *K* edge in the FeO_6 octahedron. The iron is displaced by 0.1 Å toward the apical oxygen. Full line: FDM, dotted line: MS.

the previous perfect octahedron, the apical oxygen is eliminated. The differences between FDM and MS (Fig. 9) are mainly for the polarization along Oz. The structures are thinner and the pre-edge is notably higher in the FDM calculation. The analyses of the pre-edge is a lot of used in XANES because it accompanies very often a loss of center of symmetry and because it is close to the Fermi level. A precise and quantitative evaluation of it is important and we see that it needs a full potential approach.

Planar situations frequently occurs, for instance in the new supra-conducting YBaCuO family with its CuO_2 planes. This situation is illustrated with calculations on the FeO_4 molecule where the iron is surrounded by a square of oxygen. From the previous perfect octahedron the two oxygen atoms along Oz are eliminated. The very interesting fact is that the main difference between MS and FDM is for the polarization along Oz. The peak at 10 eV is totally absent in the MS calculation (Fig. 10). The linear dichroism is used to study the CuO_2 plane in cuprate. Errors in a muffin-tin calculation can affect strongly the interpretation of the corresponding experiments.

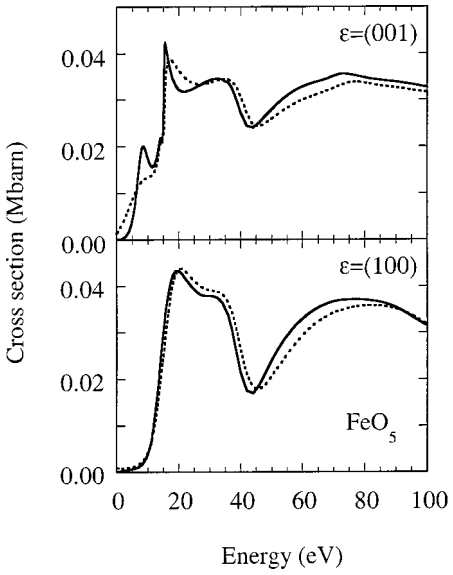

FIG. 9. Fe *K* edge in the FeO_5 molecule. The apical oxygen is missing. Interatomic distance is 2 Å. Full line: FDM, dotted line: MS.

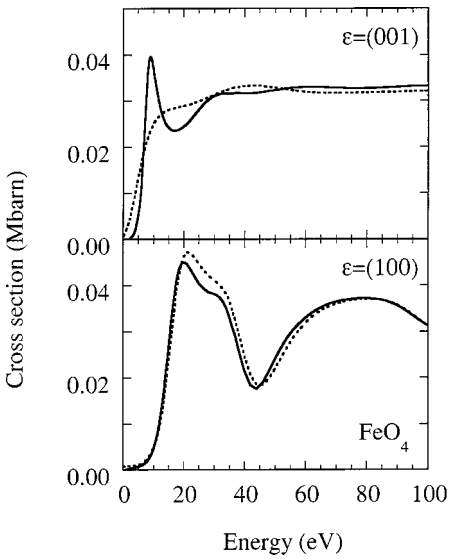

FIG. 10. Fe *K* edge in the FeO_4 planar molecule. Full line: FDM, dotted line: MS.

To illustrate a more general situation, some calculations on a FeO_2 molecule are also performed. This hypothetical molecule is taken as planar, the O–Fe–O angle being 120°. The plane is perpendicular to Oz. Figure 11 shows the linear dichroism. MS and FDM calculation are very different in all directions in the first 30 eV, especially for the polarization perpendicular to the plane of the molecule where again a peak at 8 eV is absent in the muffin-tin calculation. The actual conclusion is than in case of low symmetry, the muffin-tin MS approach is not able to calculate confidently XANES in the lower energy range.

A typical low symmetrical example: the MbCO protein

To give a real example of distorted octahedron around an iron site, the carbonmonoxy-myoglobin (MbCO) protein is chosen. Protein is an important class of material where XANES can play an important role in the determination of the local geometry around a central metallic atom. In the case of MbCO, the molecule is formed by a central iron surrounded by four pyrrole ligands that surround the heme Fe in a nearly perfect square planar symmetry.[29] Another pyrrole ligand stands beneath the plane and a CO is bonded on the other side to the central iron. Thus, the iron is surrounded by a distorted octahedra composed of six nitrogen and one carbon. An approximation of the structure where the CO is along the *Z* axis gives a C_2 symmetry.

Figure 12 presents the first step of the study of this compound with only one distorted octahedron around the iron. The difference between multiple scattering calculation and finite difference method is very strong. The FDM calculation is clearly closer to the experiment in both polarizations. For

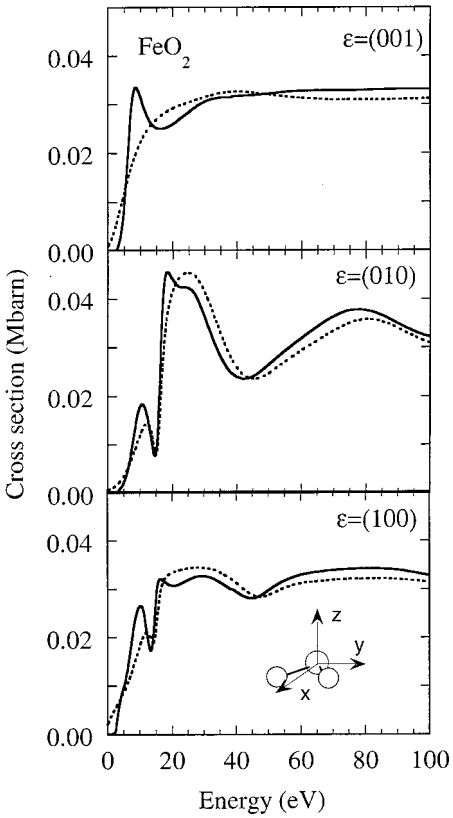

FIG. 11. Fe *K* edge in the FeO_2 molecule. The O–Fe–O bonding angle is 120°. Interatomic distances are 2 Full line: FDM, dotted line: MS.

the polarization along *z*, the double structure typical of an octahedra is transformed in a unique round structure close to the experiment.[30]

C. Discussion

From these figures it can be clearly seen that by decreasing the symmetry the discrepancy between muffin-tin and non-muffin-tin calculations become stronger. The errors in muffin-tin calculations can thus result in false interpretation of data, and thus the fit of electronic or structural parameters can converge to imprecise values. It must be also noted that the differences are mainly due to the interstitial area. Indeed, in the non-muffin-tin calculation when increasing the radii of the inner spheres using a monopolar (that is spherical) expansion of the potential, the results are only weakly affected. That means that attempts to use a multipolar expansion of the potential inside muffin-tin sphere and a constant potential between them in the MS formalism cannot be successful.

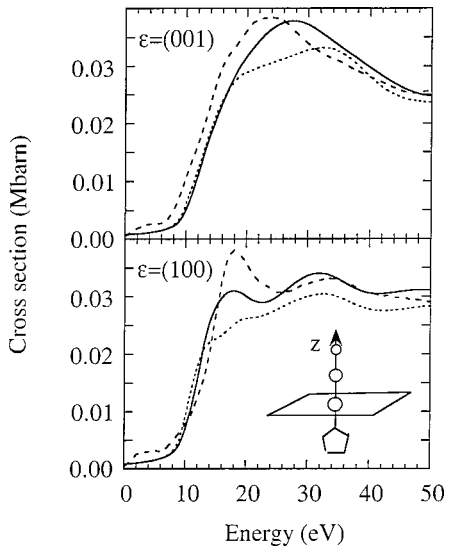

FIG. 12. Fe *K* edge in the MbCO protein. Full line:FDM, dotted line:MS, dashed line: experiment from Della Longa *et al.*[30] The molecule is in the inset. The calculation is limited to the surrounding octahedron.

VII. CONCLUSION

The main result is that the FDM is a valuable tool to calculate the XANES. The second main result is the evaluation of the accuracy of the muffin-tin approximation in the threshold area. In case of low symmetry, the muffin-tin approximation is not sufficient in the edge energy range. This can be even more crucial for anomalous diffraction spectroscopy where the signal is connected to differences between atomic form factors and so to detailed part of the atomic signal. A non-muffin-tin FDM calculation is substantially longer than a muffin-tin MS one, so the multiple scattering method should be used whenever possible and even, in any case, as a starting point. Then, in a second step, in case of low symmetry, and when the discrepancy with experiment remains too important the FDM should be used. The next step of the present work concerns the inclusion of spin effects in order to analyze the magnetic dichroism. Then, after assessing one body effect been safely realized, one should consider the many body effects.

ACKNOWLEDGMENTS

R. Natoli, D. Cabaret, and Ch. Brouder are thanked for the numerous fruitful discussions. Thanks also to S. Della Longa for his work on the MbCO structure and to B. Ravel for reading the manuscript.

[1] F. M. F. De Groot, J. Electron Spectrosc. Relat. Phenom. **62**, 111 (1993).
[2] L. F. Mattheiss and R. E. Dietz, Phys. Rev. B **22**, 1663 (1980).
[3] J. J. Rehr, S. I. Zabinsky, and R. C. Albers, Phys. Rev. Lett. **69**, 3397 (1992).
[4] T. A. Tyson, K. O. Hodgson, C. R. Natoli, and M. Benfatto, Phys. Rev. B **46**, 5997 (1992).
[5] A. Gonis, X. G. Zhang, and D. M. Nicholson, Phys. Rev. B **40**, 947 (1989).
[6] D. E. Ellis and G. S. Painter, Phys. Rev. B **2**, 2887 (1970).

[7] T. Huhne T, T. C. Zecha, H. Ebert, P. H. Dederichs, and R. Zeller, Phys. Rev. B **58**, 10 236 (1998).
[8] D. Ahlers, G. Schütz, V. Popescu, and H. Ebert, J. Appl. Phys. **83**, 7082 (1998).
[9] D. Ahlers, K. Attenkofer, and G. Schütz, J. Appl. Phys. **83**, 7085 (1998).
[10] T. Huhne and H. Ebert, Solid State Commun. **109**, 577 (1999).
[11] P. Blaha, K. Schwarz, P. Sorantin, and S. Trickey, Comput. Phys. Commun. **59**, 399 (1990).
[12] G. E. Kimball and G. H. Shortley, Phys. Rev. **45**, 815 (1934).
[13] R. M. Nieminen and M. J. Puska, Phys. Rev. Lett. **50**, 281 (1983).
[14] J. M. Thijssen and J. E. Inglesfield, Europhys. Lett. **27**, 65 (1994).
[15] Y. Joly, Phys. Rev. Lett. **68**, 950 (1992).
[16] Y. Joly, Phys. Rev. Lett. **72**, 392 (1994).
[17] Y. Joly, Phys. Rev. B **53**, 13029 (1996).
[18] E. U. Condon and G. H. Shortley, *Theory of Atomic Spectra* (Cambridge University Press, London, UK, 1953).
[19] D. Dill and J. L. Dehmer, J. Chem. Phys. **61**, 692 (1974).
[20] Y. Joly, J. Phys. IV **7**, C2-111 (1997).
[21] Y. Joly, D. Cabaret, H. Renevier, and C. R. Natoli, Phys. Rev. Lett. **82**, 2398 (1999).
[22] M. Benfatto, Y. Joly, and C. R. Natoli, Phys. Rev. Lett. **83**, 636 (1999).
[23] M. Cuozzo, Y. Joly, E. K. Hill, and C. R. Natoli, in *CP514, Theory and Computation for Synchrotron Radiation Spectroscopy*, Proceedings of the SRRTNET 99 Conference, Frascati, Italy, 1999, edited by M. Benfatto, C. R. Natoli, and E. Pace (American Institute of Physics, New York, 2000), p. 45.
[24] E. Clementi and C. Roetti, At. Data Nucl. Data Tables **14**, 177 (1974).
[25] L. Hedin and S. Lundqvist, J. Phys. C **4**, 2064 (1971).
[26] D. Cabaret, H. Renevier, Y. Joly, and C. R. Natoli, J. Synchrotron Radiat. **6**, 258 (1999).
[27] *Gaussian 94* (Revision D.1), M. J. Frisch, G. W. Trucks, H. B. Schlegel, P. M. W. Gill, B. G. Johnson, M. A. Robb, J. R. Cheeseman, T. A. Keith, G. A. Petersson, J. A. Montgomery, K. Raghavachari, M. A. Al-Laham, V. G. Zakrzewski, J. V. Ortiz, J. B. Foresman, J. Cioslowski, B. B. Stefanov, A. Nanayakkara, M. Challacombe, C. Y. Peng, P. Y. Avala, W. Chen, M. W. Wong, J. L. Andres, E. S. Replogle, R. Gomperts, R. L. Martin, D. J. Fox, J. S. Binkley, D. J. Defrees, J. Baker, J. P. Stewart, M. Head-Gordon, C. Gonzalez, and J. A. Pople (Gaussian, Inc., Pittsburgh, PA, 1995).burgh, PA, 1995).
[28] J. G. Norman, Jr., Mol. Phys. **81**, 1191 (1974).
[29] G. S. Kachalova, A. N. Popov, and H. D. Bartunik, Science **284**, 473 (1999).
[30] S. Della Longa, A. Arcovito, B. Vallone, A. Congiu Castellano, R. Kahn, J. Vicat, Y. Soldo, and J. L. Hazemann, J. Synchrotron Radiat. **6**, 1138 (1999).